

Convective heat transfer measurements in a vapour-liquid-liquid three-phase direct contact heat exchanger

Hameed B. Mahood, A. N. Campbell, Ali Sh. Baqir, A. O. Sharif & R. B. Thorpe

Heat and Mass Transfer
Wärme- und Stoffübertragung

ISSN 0947-7411

Heat Mass Transfer
DOI 10.1007/s00231-017-2260-8



Your article is protected by copyright and all rights are held exclusively by Springer-Verlag GmbH Germany, part of Springer Nature. This e-offprint is for personal use only and shall not be self-archived in electronic repositories. If you wish to self-archive your article, please use the accepted manuscript version for posting on your own website. You may further deposit the accepted manuscript version in any repository, provided it is only made publicly available 12 months after official publication or later and provided acknowledgement is given to the original source of publication and a link is inserted to the published article on Springer's website. The link must be accompanied by the following text: "The final publication is available at link.springer.com".



Convective heat transfer measurements in a vapour-liquid-liquid three-phase direct contact heat exchanger

Hameed B. Mahood^{1,2} · A. N. Campbell³ · Ali Sh. Baqir⁴ · A. O. Sharif³ · R. B. Thorpe³Received: 10 July 2017 / Accepted: 21 December 2017
© Springer-Verlag GmbH Germany, part of Springer Nature 2017

Abstract

Energy usage is increasing around the world due to the continued development of technology, and population growth. Solar energy is a promising low-grade energy resource that can be harvested and utilised in different applications, such as solar heater systems, which are used in both domestic and industrial settings. However, the implementation of an efficient energy conversion system or heat exchanger would enhance such low-grade energy processes. The direct contact heat exchanger could be the right choice due to its ability to efficiently transfer significant amounts of heat, simple design, and low cost. In this work, the heat transfer associated with the direct contact condensation of pentane vapour bubbles in a three-phase direct contact condenser is investigated experimentally. Such a condenser could be used in a cycle with a solar water heater and heat recovery systems. The experiments on the steady state operation of the three-phase direct contact condenser were carried out using a short Perspex tube of 70 cm in total height and an internal diameter of 4 cm. Only a height of 48 cm was active as the direct contact condenser. Pentane vapour, (the dispersed phase) with three different initial temperatures (40 °C, 43.5 °C and 47.5 °C) was directly contacted with water (the continuous phase) at 19 °C. The experimental results showed that the total heat transfer rate per unit volume along the direct contact condenser gradually decreased upon moving higher up the condenser. Additionally, the heat transfer rate increases with increasing mass flow rate ratio, but no significant effect on the heat transfer rate of varying the initial temperature of the dispersed phase was seen. Furthermore, both the outlet temperature of the continuous phase and the void fraction were positively correlated with the total heat transfer rate per unit volume, with no considerable effect of the initial temperature difference between the dispersed and continuous phases.

Nomenclature

H_o	Water level in the test section (m).
\dot{m}_c	Continuous phase mass flow rate (kg/min).
\dot{m}_d	Dispersed phase mass flow rate (kg/min).
R	Mass flow rate ratio.
Q_v	Heat transfer rate per unit volume (kW/m ³).
U_v	Volumetric heat transfer coefficient (kJ/m ³ .s).
T_{ci}	Continuous phase inlet (initial) temperature (°C).

T_{co}	Continuous phase outlet temperature (°C)
T_{cond}	Temperature of the condensate (°C)
T_{c1-4}	Local temperature (position 1 to 4) along the test section height (°C)
T_{di}	Dispersed phase inlet (initial) temperature (°C)
ΔT_{lmi}	Log-mean temperature difference of section (i) of the test section (°C)

Subscript

c	Continuous phase
d	Dispersed phase
i	Initial (or inlet)
o	Outlet

✉ Hameed B. Mahood
hbmahood@yahoo.com

- ¹ Department of Science, University of Misan, Misan, Iraq
- ² College of Applied Science, Department of Engineering/ Chemical Engineering, Sohar, Oman
- ³ Department of Chemical and Process Engineering, Faculty of Engineering and Physical Sciences, University of Surrey, Guildford GU2 7XH, UK
- ⁴ Engineering Technical College, Al-Furat Al-Awsat Technical University, Al-Najaf 31003, Iraq

1 Introduction

The global energy situation is getting worse due to the reduction in fuel supplies, and increasing fuel costs. Nevertheless, the demand for energy will continue to increase because of the advancement of technologies in developing countries and

continued population growth. Fossil fuels are still the main energy source, providing about 80% of the global net energy requirement, while renewable energy contributes only 11% [1]. Accordingly, environmental problems, such as global warming and air pollution will continue to increase. For these reasons, it is important to seek new and more efficient energy resources.

The utilisation of low-grade energy resources, such as those that harvest direct solar energy (*e.g.* solar ponds and solar water heaters) are promising and have recently received more attention [2]. In both systems, direct solar radiation is commonly converted to thermal energy, where the solar radiation is absorbed by a body of water in the former, or directed to heat a stream of fluid, which can be used later in another heat extraction process, in the latter.

In solar heater applications, the exchange can be achieved by flowing air under an absorbing surface in a configuration like a surface type heat exchanger. However, a high heat transfer resistance could impede the flow of heat from the absorbing surface to the flowing air that is used as a working fluid [3]. Consequently, the efficiency of the heat transfer process is reduced, making it impractical. In another design, a surface type heat exchanger is used to transfer the heat absorbed by a working fluid to a water storage tank. The heat exchanger should be manufactured from highly conductive materials, such as steel, aluminium and copper. Different configurations of the heat exchanger have been designed, but an immersed coil in the storage tank, the shell and tube heat exchanger and the mantle heat exchanger are the most widely used [2]. The main obstacle still facing the exploitation of such low-grade energy resources is the low efficiency of the equipments (mainly the heat exchangers) that are used in the recovery processes. The capital cost of these units, especially the heat exchangers, is another reason. To overcome these obstacles, a direct contact heat transfer process between two immiscible fluids utilising sensible heat transfer has been suggested, such as that studied by Hyun *et al.* [4]. In this process, the working fluid could be lighter or heavier than water, but it must be completely immiscible with water. In the case of a heavier working fluid, the distributor is fixed at the top of the exchanger and *vice versa*.

The spray column direct contact heat exchanger is suitable for this application because it does not require adjustment of the liquid-liquid interface as in coalescence devices containing packing materials [4]. Figure 1 shows two possible configurations of a hot water heater utilising a direct contact heat exchanger with no phase change of working fluid.

Because the configurations discussed above are based on the principle of the transfer of sensible heat (*i.e.* with no phase change) between the working fluid (heating media) and water, the heat transfer efficiency of these configurations is low. This is because the heating process needs a high mass flow rate of

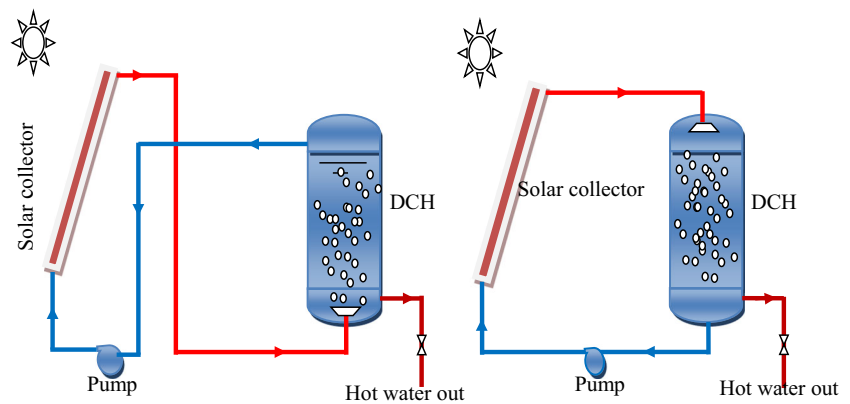
working fluid and hence a large exchanger size, which increases the cost of the process. Therefore, the use of a working fluid that is completely immiscible with water, and has low or relatively low boiling point could enhance the heat transfer process by utilising the latent heat in addition to the sensible heat. This can reduce the volume of working fluids needed by orders of magnitude, making the process more economically attractive. Furthermore, Peng *et al.* [5] claimed that the heat transfer coefficient for direct contact heat transfer between two immiscible fluids with a phase change could be greater than that of a single phase by 20–200 times. Thus, the working fluid could be condensed in a water column or tank after being vaporised in a suitable solar collector. The rapid heat transfer should increase the water outlet temperature and reduce the heating time. From this point of view, the assessment of the direct contact condenser under different operational conditions becomes important for developing an efficient heat transfer process utilising the solar energy.

In contrast to a conventional surface type heat exchanger, such as the shell and tube heat exchanger, the contacting fluids in the direct contact heat exchanger come into intimate physical contact. Therefore, it has a high heat transfer rate, an absence of corrosion and fouling problems, a lower cost, a simple design and has the potential to work with a very low temperature driving force ($\Delta T \approx 1^\circ\text{C}$). Accordingly, they can potentially be exploited in many other applications, such as water desalination, geothermal power generation, and nuclear reactor safety [6].

Depending on the purpose of the heat transfer process the three-phase direct contact heat exchanger can be designed as an evaporator or a condenser. Attention has been mostly directed toward the three-phase direct contact evaporator rather than the condenser (see [7–10]). There is therefore a distinct lack of mathematical design equations, or even experimental data on the three-phase direct contact condenser. The direct contact condensation of a single bubble in an immiscible liquid, which represents the basis of the three-phase direct contact condenser, has been researched widely [11–17]. However, only very few studies can be found regarding multi-bubble [18–21] systems, and bubble-trains [22]. These are of course more representative of a real direct contact condenser.

Recently, Mahood *et al.* have investigated extensively the heat transfer characteristics of the three-phase direct contact condenser, both experimentally and theoretically. The effect of various operational parameters, such as the mass flow rates of both the continuous and dispersed phases and the initial temperature of the dispersed phase on the different heat transfer parameters, such as the axial steady state [23, 24] and transient temperature distributions [25]. Additionally, the volumetric heat transfer coefficient in transient [26] and steady-state operation [27, 28] of the condenser was examined. The heat

Fig. 1 Liquid-liquid (sensible heat transfer) direct contact heat exchanger arrangement for solar water heating [4]



transfer efficiency and capital cost of the condenser [29] and reverse flow limitation [30, 31] were calculated. These works have not however reported the heat flux associated with the condensation of the bubbles in the direct contact condenser.

In this paper, the heat transfer rate per unit volume of the three-phase direct contact condenser is studied experimentally. The effects of different operational parameters, such as the mass flow rate ratio, initial temperature of the dispersed phase (working fluid) and the working fluid void fraction, on the total heat transfer rate per unit volume of the condenser are investigated. In addition, the total heat transfer rate per unit volume along the condenser height is studied.

2 Experimental setup and procedure

A detailed description of the experimental setup and the experimental procedure can be found in the previous published work [29, 30]. In outline, the experimental set up is shown in Fig. 2. In addition to a direct contact condenser (test section), it includes two loops. The first loop is a dispersed phase circulation loop. It consists of a small liquid pentane storage tank, a vaporisation vessel, a circulation pump, ball valves, a non-return valve, a pressure gauge and connection pipes. The second, continuous phase consists of a large water storage tank, a pump, flow meters and connection pipes. Furthermore, eight calibrated thermocouples were used to measure the temperature distribution along the test section (condenser), the temperature of the water at the inlet, the condensate, and the temperature of the dispersed phase at its injection point into the test section. Tap water and high purity n-pentane were used as the continuous phase and the dispersed phase, respectively. The vaporising vessel is a large pool type vaporiser with a long copper coil for carrying and vaporising the dispersed phase.

The set of experiments began with the preparation of the continuous phase (19°C). The large storage tank and short duration of an individual experimental run helped to

maintain the temperature of the continuous phase at a constant value. Concomitantly, the heating vessel was warmed by increasing the electrical power to the two heaters (3 kW each) gradually until the desired temperature was reached. Liquid pentane was pumped from its storage tank to the coil of the vaporising vessel. Liquid pentane was vaporised in the coil, and injected into the direct contact test section when it reached the desired temperature via a short externally heated pipe (by a trace heater), a calibrated injection valve, and sparger. The injection pressure and the vapour temperature were measured using a pressure gauge and a thermocouple. At the moment of vapour injection, the temperature distribution along the direct contact test section was measured and read directly on a PC using an 8 channel data logger. Due to gravity, the condensate formed after each run as a separated layer at the top of the test section. It was collected and sent back to the liquid pentane storage tank during continuous operation, or stored and used in another run in batch mode. A separating conical flask was used for separating the condensate (if any) from the draining water. The dispersed phase mass flow rate was calculated using a mass balance for each individual run. The collected condensate (liquid pentane) was weighted and divided by the run duration. The initial conditions of the experiments are shown in Table 1. The uncertainty of the thermocouple measurements is given in Table 2. The total error in the measurements has also been calculated. The inaccuracy of the dispersed phase mass flow rate was estimated and found to be about $\pm 11\%$.

3 Results and discussion

A calculation of the total heat transfer rate per unit volume throughout a three-phase direct contact condenser has been carried out. The calculation is based on the experimental axial temperature measurements, and the previous experimental values of volumetric heat transfer coefficient [27].

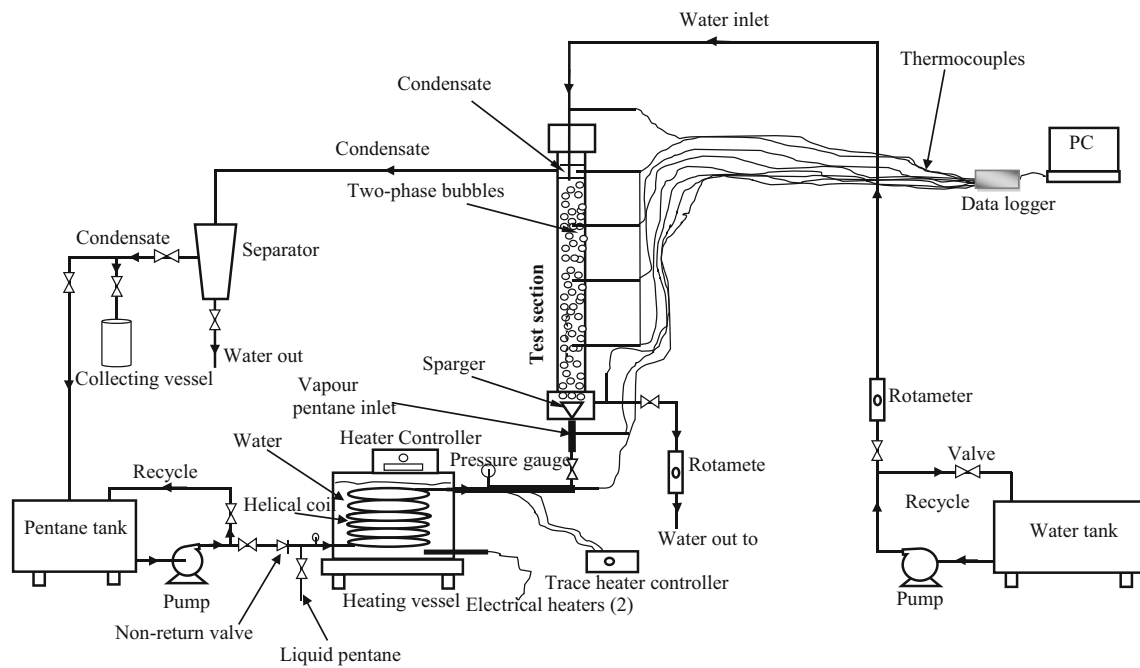


Fig. 2 Schematic diagram of the experimental rig

Direct contact condensation utilising bubbles or drops offers a large interfacial heat transfer area, and in general, the heat exchange process through this area takes place by convection. Hence, the heat rate can be found via the well-known formula:

$$Q_{vi} = U_{vi} \Delta T_{lmi} \quad (1)$$

Where Q_{vi} , V_i , U_{vi} and ΔT_{lmi} denote, for a sub-volume, the total heat transfer rate per volume, the direct contact volumetric heat transfer coefficient, and the log-mean temperature difference, respectively.

The axial distribution of the total heat transfer rate per unit volume along the column, for three different initial dispersed phase temperatures is shown in Figs. 3, 4 and 5). In all cases, the total heat transfer rate per unit volume, (independent of the mass flow rate) falls from its highest value at the dispersed phase inlet towards the top of the heat exchanger. This could be attributed to the fact that close to the injection point, the hot vapour bubbles move with a higher velocity due to the buoyancy force. Here, the density of the bubbles is minimal and the injection pressure is still effective. The density of the bubbles

Table 1 The initial conditions of the experiments

$T_{di} (^{\circ}\text{C})$	$T_{ci} (^{\circ}\text{C})$	$H_o(\text{m})$	$\dot{m}_c (\frac{\text{kg}}{\text{min}})$	$R = \frac{\dot{m}_i}{\dot{m}_c} \times 100\%$				
40	19	0.48	0.05	16.00	31.00	49.60	58.50	66.60
			0.1	11.00	14.00	18.20	22.40	32.60
			0.2	7.30	10.00	13.70	14.80	19.00
			0.28	5.40	7.50	9.00	10.50	14.30
			0.38	4.80	6.00	7.40	8.40	9.40
43.5	19	0.48	0.05	15.30	11.50	8.10	4.80	4.00
			0.1	29.00	17.30	9.40	7.50	4.50
			0.2	37.20	25.60	11.40	8.80	5.00
			0.28	41.60	26.70	14.20	10.50	6.80
			0.38	52.70	30.00	18.60	14.00	8.40
47.5	19	0.48	0.05	3.90	5.70	7.70	11.30	13.20
			0.1	4.70	8.70	9.50	11.60	12.60
			0.2	7.90	10.60	15.60	17.70	19.30
			0.28	11.60	16.90	22.90	26.70	28.60
			0.38	25.40	30.30	35.50	45.20	54.40

Table 2 Inaccuracy of the thermocouples

$T(^{\circ}C)$	Inaccuracy %
T_{e1}	± 0.4
T_{e2}	± 0.5
T_{e3}	± 0.3
T_{e4}	± 0.3
T_{cond}	± 0.6
T_{di}	± 0.5
T_{ci}	± 0.3

will increase with condensation progressing along the column since the condensate accumulates within the bubbles. Hence the upward bouyancy force declines and thus the bubbles will decelerate. A very thin boundary layer forms around the bubbles, i.e. there is a low heat transfer resistance, at this stage (bottom of the column) and it extends over the whole surface of the bubble, while the bubble condenses which results in further deceleration [19].

The temperature difference between the two phases is another important reason that could account for the observed behavior of the rate of heat transfer per unit volume over the column height. The temperature difference, actually, represents the driving force for the heat exchange process between the two phases in the direct contact column. Practically, its maximum value can only be achieved at the bottom of the column and it will decrease with the column height due to the cooling effect produced by the direct contact between of the vapour bubbles and the subcooled continuous phase. Rapid heat exchange can take place at the bottom of the column and it gradually slows down along the column.

A considerable part of the total heat transfer occurs during the two-phase bubble formation period [32], which is included in this lower section of the column. It is unsurprising therefore that a decrease in the total heat transfer per unit volume occurs directly after the bubbles have passed through the first part of the column.

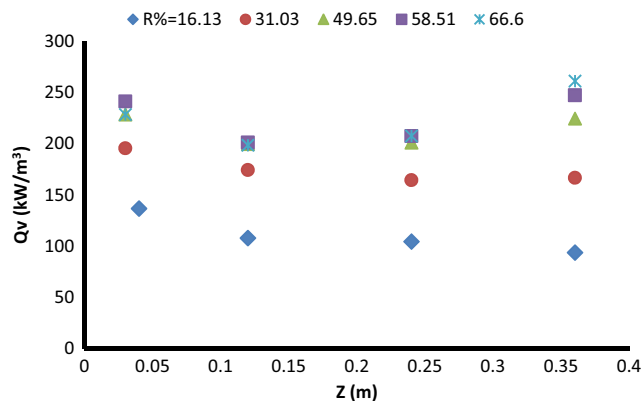


Fig. 3 Total heat transfer rate per unit volume along the direct contact condenser height for $T_{di}=40^{\circ}C$, continuous phase mass flow rate ($\dot{m}_c = 0.05$ kg/min) and five different mass flow rate ratios

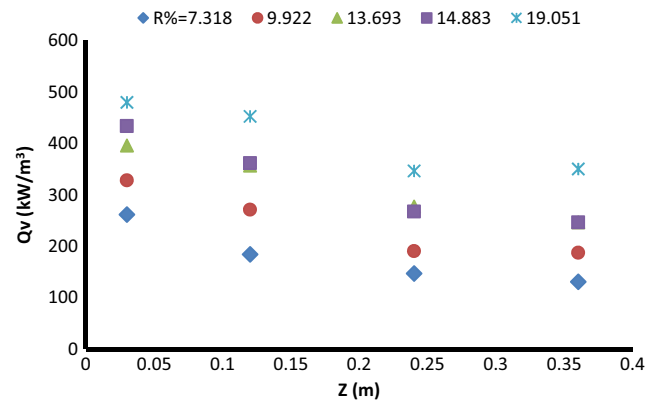


Fig. 4 Total heat transfer rate per unit volume along the direct contact condenser height for $T_{di}=40^{\circ}C$, continuous phase mass flow rate ($\dot{m}_c = 0.2$ kg/min) and five different mass flow rate ratios

Depending on the continuous phase mass flow rate, there are then three distinct behaviours of the total heat transfer rate per unit volume at the second half of the column, as can be seen in Figs. 3, 4 and 5). For low continuous phase mass flow rates ($\dot{m}_c = 0.05$ kg/min) the (Q_v) decreases as described above to reach its lowest value at a position near at the middle of the column. The heat transfer rate then increases towards the top of the column (see Fig. 3). This behaviour of the (Q_v) clearly also depends strongly on the dispersed phase mass flow rate, or the mass flow rate ratio (R). The curvature in the profile of the heat transfer rate is more pronounced at a high dispersed phase mass flow rate (or high R), with the profiles flattening out significantly as the dispersed mass flow rate (or R) is decreased. At high mass flow rate ratios (i.e. high dispersed phase mass flow rates and low continuous phase mass flow rates), the condensation of vapour in the bubbles is not completed through the first half the column. Therefore the two-phase (vapour-liquid) bubbles formed still exist until they reach the last part of the column due to inadequate cooling phase or continuous phase being available. Therefore, the uncondensed vapour in the two-phase (vapour-liquid)

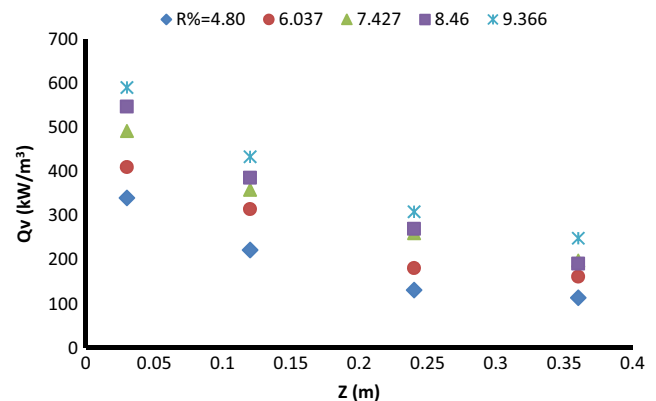


Fig. 5 Total heat transfer rate per unit volume along the direct contact condenser height for $T_{di}=40^{\circ}C$, continuous phase mass flow rate ($\dot{m}_c = 0.38$ kg/min) and five different mass flow rate ratios

bubbles, which still has latent heat, could be liberated due to further condensation in the upper region of the column where the continuous phase is at its coolest. Furthermore, bubble-bubble interactions in the upper part of column, which takes place due to the deceleration of the two-phase bubbles because of the recuduction in buoyancy forces, could result in enhanced heat transfer. The probability of interactions is increased with increasing two-phase bubble size, which is expected to occur at high dispresed phase mass flow rates. Therefore, the two-phase bubbles will break down and split into smaller separated vapour bubbles and liquid drops. This would result in a distortion of the boundary layer and an increase in interfacial area thereby allowing further condensation by direct contact with the cooling liquid.

At a moderate continuous phase mass flow rate ($\dot{m}_c = 0.2 \text{ kg/min}$), the (Q_v) decreases slightly upon moving from the bottom to the top of the column (see Fig. 4). Only at the highest dispersed phase mass flow rate considered ($\dot{m}_d = 0.038 \text{ kg/min}$ or $R = 19\%$) does the (Q_v) increase over the second half of the column. Even then, the effect is very small. As above, the dispersed phase mass flow rate (or R) seems to significantly affect the value of (Q_v) . The higher the dispersed phase mass flow rate (R), the higher the (Q_v) due to the increased heat load being carried in by the bubbles.

Finally, at higher continuous phase mass flow rates ($\dot{m}_c = 0.38 \text{ kg/min}$), generally the (Q_v) decreases with the column height for all of the dispersed phase mass flow rates studied (see Fig. 5). This could be reasonably justified by insufficient dispersed phase (heating media) being present, in comparison with the continuous phase (cooling media).

The dependancy of the heat transfer rate per unit volume on the mass flow rate ratios (variable dispersed phase mass flow rate to a constant continuous phase mass flow rate), for three different initial temperatures of the dispersed phase is shown in Figs. 6, 7 and 8). It is clear from these plots that the higher the mass flow rate ratio, the higher is the heat transfer rate per

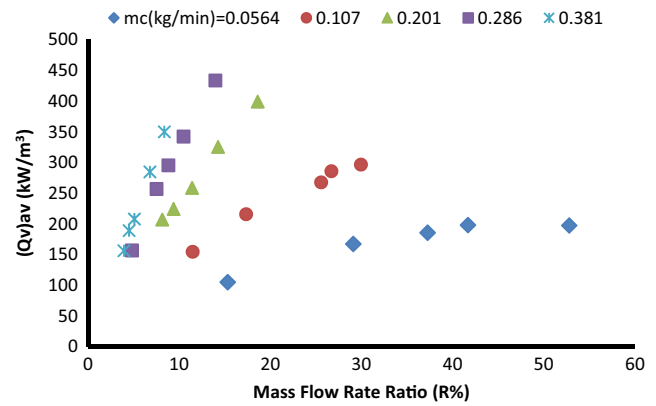


Fig. 7 Heat transfer rate per unit volume versus mass flow rate ratio for initial temperature of the dispersed phase ($T_{di} = 43.5^\circ\text{C}$) and five different continuous phase mass flow rates

unit volume. This could be explained by the fact that the higher the mass flow rate ratio contributes to an abundance of the heat source (hot vapour bubbles) in the column. Consequently, there is an increase in the magnitude of the exchange of heat between the two direct contact phases.

Additionally, it is also clear that when the continuous phase mass flow rate is increased, so too does the heat transfer rate per volume. This could be simply justified by the fact that with an adequate amount of the cooling phase in the column, the condensation process will be improved. So, this improvement would definitely result in a high energy transfer as heat between the contacting phases. What is also noteworthy is that the improvement in heat transfer rate per unit volume as the continuous phase flow is increased diminishes at higher mass flow rates. It is evident from all three figures that the difference between the highest two continuous phase flowrates shown is almost negligible. This could be attributed to the complete condensation of vapour bubbles by an adequate amount of cooling phase, with any further cooling provided by additional continuous phase having little effect on the overall performance, as it only removes sensible heat.

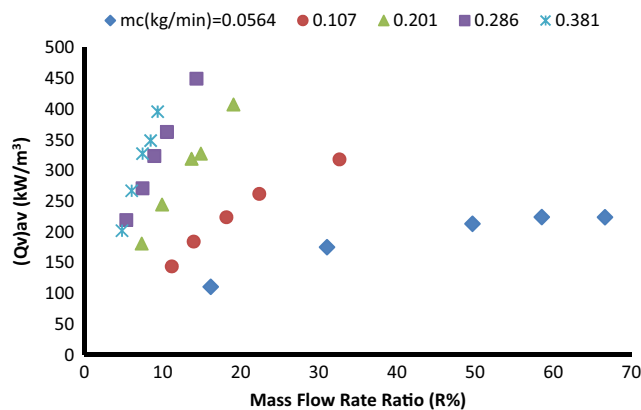


Fig. 6 Heat transfer rate per unit volume versus mass flow rate ratio for initial temperature of the dispersed phase ($T_{di} = 40^\circ\text{C}$) and five different continuous phase mass flow rates

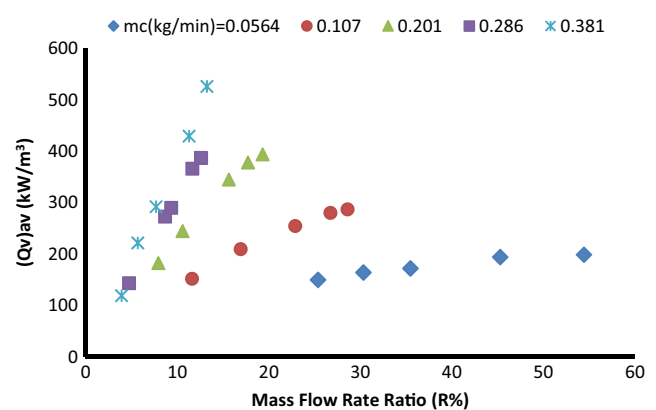


Fig. 8 Heat transfer rate per unit volume versus mass flow initial temperature of the dispersed phase ($T_{di} = 47.5^\circ\text{C}$) and five different continuous phase mass flow rates

Figure 9 shows the variation of the total heat transfer per unit volume with the initial temperature difference between the dispersed and continuous phases, for four different dispersed phase mass flow rates. It is clear from the figure that the total heat transfer decreases slightly upon increasing the initial temperature difference. A high-dispersed phase flow rate clearly resulted in an increase in the total heat transfer per unit volume of the condenser. This is of course unsurprising given that there is more heating medium present in the system, and also greater mixing due to the higher injection velocity and number of bubbles. The amount of thermal energy that can therefore be absorbed by the cooling phase (continuous phase) as a result of the condensation of the bubbles is high. Furthermore, Fig. 9, indicates that the total heat transfer rate per unit volume is slightly decreased when the initial temperature difference between the two phases is increased. In the present experiments, the initial temperature difference between the two phases was achieved by varying the initial temperature of the dispersed phase whilst the initial temperature of the continuous phase was held constant. However, the increase of the initial temperature of the dispersed phase (bubbles) could result in a high condensation rate even during bubble formation. Two-phase bubbles are immediately formed at the sparger just after the dispersed vapour first touches the continuous phase and the liquid condensate then accumulates in the bubbles.

Figures 10 and 11) illustrate the variation of the total heat transfer rate per unit volume with the continuous phase outlet temperature for three different initial temperatures of the dispersed phase. In general, the heat transfer rate increases with increasing the continuous phase outlet temperature and decreases with increasing the initial temperature of the dispersed phase. This supports the hypothesis, discussed previously, that latent heat dominates the direct contact condensation process [23]. The higher outlet temperature of the continuous phase indicates for a good heat transfer process. Therefore, the

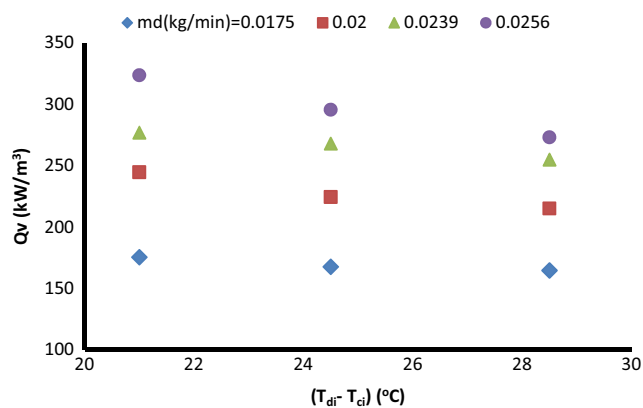


Fig. 9 Total heat transfer rate per unit volume versus initial temperature difference between the dispersed and continuous phases, for four different dispersed phase mass flow rates

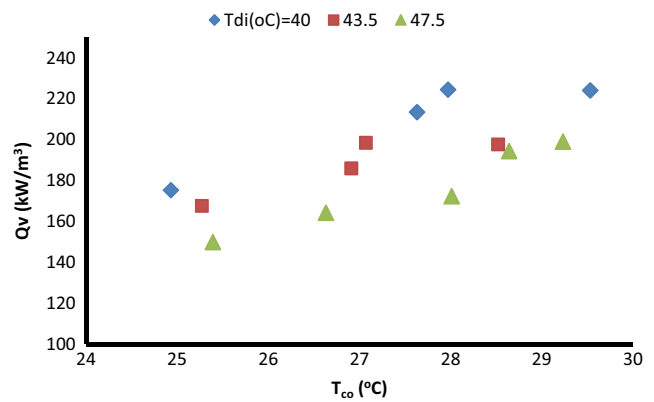


Fig. 10 Heat transfer rate per unit volume versus continuous phase outlet temperature, for a continuous phase mass flow rate ($\dot{m}_c = 0.05 \text{ kg/min}$) and three different initial temperatures of the dispersed phase

amount of energy transferred through the direct contact condensation process is high. Furthermore, a lower initial temperature of the dispersed phase has a slight effect the direct contact condensation. The lower the initial dispersed phase temperature, the higher the heat transfer is. This is in complete agreement with the basic knowledge of convective heat transfer mechanisms as the temperature driving force for condensation is larger.

The effect of the void fraction on the heat transfer rate per unit volume for three different dispersed phase initial temperature is shown by Figs. 12 and 13). It is clear that the total heat transfer rate increases almost linearly with the void fraction with a slight effect of the dispersed phase initial temperature. This could be justified by the fact that the increase in the void fraction is a result of an increasing in the heating medium in the condenser, which enhances the heat exchange process. In addition, the increase in void fraction leads to a slowing of the rise velocity of the bubbles and hence an increase in the bubble residence time in the heat exchanger. The bubble-bubble interaction will also increase which results in bubble fragmentation or splitting. Thus, the surface area of the bubbles that is

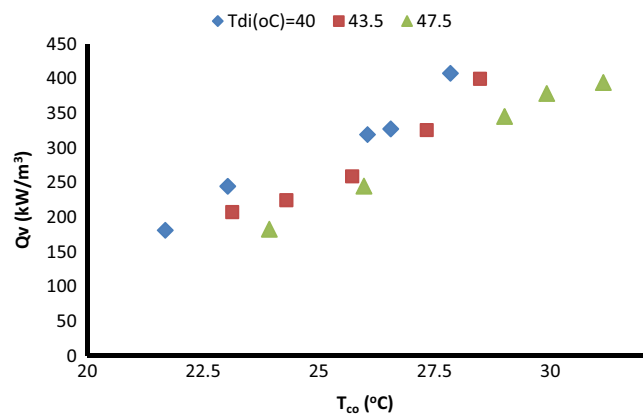


Fig. 11 Heat transfer rate per unit volume versus continuous phase outlet temperature, for a continuous phase mass flow rate ($\dot{m}_c = 0.2 \text{ kg/min}$) and three different initial temperatures of the dispersed phase

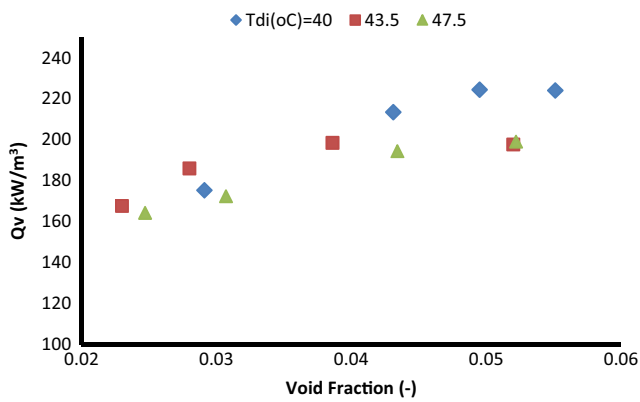


Fig. 12 Heat transfer rate per unit volume versus holdup ratio, for a continuous phase mass flow rate ($\dot{m}_c = 0.1\text{kg/min}$) and three different initial temperatures of the dispersed phase

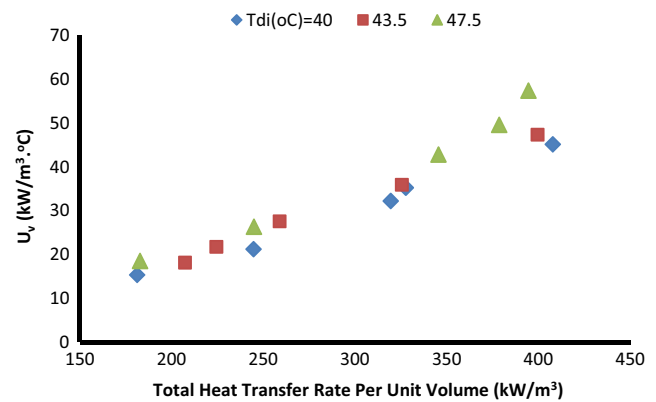


Fig. 14 Variation of volumetric heat transfer coefficient at the condenser outlet with total heat transfer rate per unit volume for three different dispersed phase initial temperature and $\dot{m}_c = 0.2\text{kg/min}$

exposed to heat exchange is increased and so and more latent heat will be liberated by enhancing the direct condensation. Accordingly, the heat transfer rate is increased.

The uncertainty in the heat transfer rate per unit volume was calculated in a manner similar to [33] and it was found that, in general, it was more than the systematic error of the thermocouples. The maximum uncertainty in the (Q_v) measurements were ± 4.3 at $R = 7.3\%$ when $\dot{m}_c = 0.2\text{ kg/min}$.

Finally, the volumetric heat transfer coefficient indicates how the heat transfer process is efficient. It is well known that the volumetric heat transfer coefficient of the the three-phase direct contact heat exchanger is much more than that of the single phase surface heat exchanger. However, different parameters can affect the volumetric heat transfer coefficient of the three-phase bubble type heat exchanger. Most of these parameters have been previously studied by Mahood et al. [21, 23–30]. Thus, the volumetric heat transfer coefficient as a function of the total heat transfer rate per unit volume for three different dispersed phase initial temperatures is shown by Fig. 14. It is clear that the volumetric heat transfer coefficient

of the condenser increases almost linearly with the total heat transfer rate. This behaviour is expected according to the expression describes this relationship, which is simply represented by Eq. (1) above. This can be simply justified by the fact that the high heat transfer rate refers to an efficient heat exchange process and hence a higher value of the coefficient.

A very slight effect of the dispersed phase initial temperature on the volumetric heat transfer coefficient can be shown, especially at a high total heat transfer per unit volume. This confirms our previous conclusion that the latent heat is dominant throughout the direct contact condensation process.

4 Conclusions

The total heat transfer rate per unit volume in a three-phase direct contact condenser has been measured experimentally to investigate the possibility of using it in solar energy applications, specifically a solar water heater. According to the results, the following useful conclusions can be made:

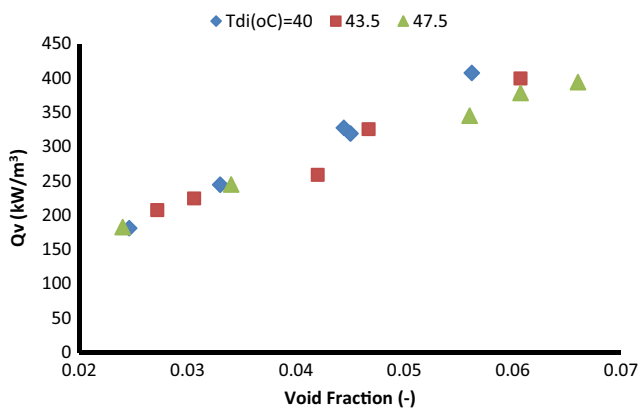


Fig. 13 Heat transfer rate per unit volume versus holdup ratio, for a continuous phase mass flow rate ($\dot{m}_c = 0.2\text{kg/min}$) and three different initial temperatures of the dispersed phase

- The direct contact condensation process is an efficient heat transfer process as a result of eliminating the barrier heat transfer resistance.
- The direct contact condensation process is a latent heat dominant process, which gives an indication that the initial temperature of the vapour dispersed phase has no significant effect on the process efficiency. This is completely different from a sensible heat transfer process, such as that used by Hyun et al. [4] for a solar heater application, where the initial temperature of the dispersed phase is the key parameter for the process.
- The direct contact heat transfer process is achieved with a low dispersed phase mass flow rate. This reflects positively on the capital cost of the process by reducing the pumping cost.

References

- Chen Y (2006) Novel cycles using carbon dioxide as working fluid. Licenciate thesis, School of Engineering and Management, Stockholm
- Shukla R, Sumathy K, Erickson P, Gong J (2013) Recent advances in the solar water heating systems: A review. *Renewable and Sust Ener Reivew* 19:173–190
- Acir A, Ata I (2016) A study of heat transfer enhancement in a new solar air heaters having circular type turbulators. *J Energy Inst* 89(4):606–616
- Hyun Y, Hyun J, Chun W, Kang Y (2005) An experimental investigation into the operation of a direct contact heat exchanger for solar exploitation. *Int Commun Heat Mass Transfer* 32(3):425–434
- Peng Z, Yiping W, Cuili G, Kun W (2001) Heat transfer in gas–liquid–liquid three-phase direct-contact exchanger. *Chem Eng J* 84(3):381–388
- Dammel F, Beer H (2003) Heat transfer from a continuous liquid to an evaporating drop: a numerical analysis. *Int J Therm Sci* 42(7): 677–686
- Hewitt G, Shires G, Bott T (1994) *Process heat transfer*. CRC Publication, New York
- Mahood HB (2016) Experimental and theoretical investigation of a three-phase direct contact condenser. PhD Thesis, Department of Chemical and Process Engineering, University of Surrey
- Baqir AS, Mahood HB, Campbell AN, Griffiths AJ (2016) Measuring the average volumetric heat transfer coefficient of a liquid–liquid–vapour direct contact heat exchanger. *Appl Therm Eng* 103:47–55
- Baqir AS, Mahood HB, Hamed MS, Campbell AN (2016) Heat transfer measurement in a three-phase spray column direct contact heat exchanger for utilization in energy recovery from low-grade sources. *Energy Convers Manag* 126:342–351
- Sideman S, Hirsch G (1965) Direct contact heat transfer with change of phase: Condensation of single vapor bubbles in an immiscible liquid medium. Preliminary studies. *AICHE J* 11(6):1019–1025
- Isenberg J, Sideman S (1970) Direct contact heat transfer with change of phase: bubble condensation in immiscible liquids. *Int J Heat Mass Transf* 13(6):997–1011
- Moalem D, Sideman S (1973) The effect of motion on bubble collapse. *Int J Heat Mass Trans* 16(12):2321–2329
- Higeta K, Mori Y, Komotori K (1979) Condensation of a single vapor bubble rising in another immiscible liquid. *AIChES ymp* 75(189), San Diego: 256–265
- Kalman H, Mori Y (2002) Experimental analysis of a single vapor bubble condensing in subcooled liquid. *Chem Eng J* 85(2):197–206
- Kalman H (2003) Condensation of bubbles in miscible liquids. *Int J Heat Mass Trans* 46(18):3451–3463
- Mahood HB (2016) Convective Heat Transfer to an Evaporating Liquid Drop in a Direct Contact with an Immiscible Liquid: Theoretical Analysis for Heat Transfer Coefficient and Bubble Growth Rate. *Int J Eng Res* 5(9):783–786
- Moalem D, Sideman S, Orell A, Hetsroni G (1973) Direct contact heat transfer with change of phase: condensation of a bubble train. *Int J Heat Mass Transf* 16(12):2305–2319
- Kalman H (2006) Condensation of a bubble train in immiscible liquids. *Int J Heat Mass Trans* 49(13):2391–2395
- Mahood HB, Sharif A, Al-alibi S, Hussini SA, Thorpe RB (2016) Thorpe, Heat transfer modelling of two-phase bubbles swarm condensing in three-phase direct-contact condenser. *J Thermal Science* 20(1):143–153
- Mahood HB, Campbell AN, Thorpe RB, Sharif A (2015) A new model for the drag coefficient of a swarm of condensing vapour–liquid bubbles in a third immiscible liquid phase. *Chem Eng Sci* 131:76–83
- Sideman S, Moalem D (1974) Direct contact heat exchangers: comparison of counter and co-current condensers. *Int J Multiphase Flow* 1(4):555–572
- Mahood HB, Sharif A, Al-Alibi S, Hawkins D, Thorpe RB (2014) Analytical solution and experimental measurements for temperature distribution prediction of three-phase direct-contact condenser. *Energy* 67:538–547
- Mahood HB, Thorpe RB, Campbell AN, Sharif A (2015) Effect of various parameters on the temperature measurements in a three-phase direct contact condenser. *Int J Therm Tech* 5(1):23–27
- Mahood HB, Thorpe RB, Campbell AN, Sharif A (2015) Experimental measurements and theoretical prediction for the transient characteristic of a three-phase direct contact Condenser. *Appl Therm Eng* 87:161–174
- Mahood HB, Sharif A, Thorpe RB (2015) Transient volumetric heat transfer coefficient prediction of a three-phase direct contact condenser. *Heat Mass Trans* 52(2):165–170
- Mahood HB, Campbell AN, Thorpe RB, Sharif A (2015) Experimental measurements and theoretical prediction for the volumetric heat transfer coefficient of a three-phase direct contact condenser. *Int Commun Heat Mass Transfer* 66:180–188
- Mahood HB, Campbell AN, Sharif A, Thorpe R (2017) B (2017) Measuring the Overall Volumetric Heat Transfer Coefficient in a Vapour-Liquid-Liquid Three-Phase Direct Contact Heat Exchanger. *Heat Transfer Eng.* <https://doi.org/10.1080/01457632.2017.1295736>
- Mahood HB, Campbell NA, Thorpe RB, Sharif A (2015) Heat transfer efficiency and capital cost evaluation of a three-phase direct contact heat exchanger for the utilisation of low-grade energy sources. *Energy Convers Manag* 106:101–109
- Mahood HB, Campbell AN, Sharif A, Thorpe RB (2016) Heat transfer measurement in a three-Phase direct-contact condenser under flooding conditions. *Appl Therm Eng* 95:106–114
- Mahood HB, Campbell AN, Thorpe RB, Sharif A (2016) Flooding Limitation in a Three-Phase Direct Contact Condenser for the Utilisation in Low-Grade Energy Resources. *ARC'16, Doha, Qatar, March.* <https://doi.org/10.5339/qfarc.2016.EESP2740>
- Chen WB, Tan RB (2003) Theoretical analysis of two-phase bubble formation in an immiscible liquid. *AICHE J* 49(8):1964–1971
- Coleman HW, Steele WC (1999) *Experimentation and Uncertainty Analysis for Engineers*. John Wiley & Sons, New York